ARCHIVES OF ELECTRICAL ENGINEERING VOL. 65(2), pp. 349-360 (2016)

DOI 10.1515/aee-2016-0026

The influence of impurities on the operation of selected fuel ignition systems in combustion engines

SEBASTIAN RÓŻOWICZ, SZYMON TOFIL

Kielce University of Technology
25-314 Kielce, al. Tysiąclecia Państwa Polskiego 7, Poland
e-mails: s.rozowicz@tu.kielce.pl, tofil@tu.kielce.pl

(Received: 10.06.2015, revised: 28.02.2016)

Abstract: The paper attempts to determine the impact of fuel impurities on the spark discharge energy and the wear of the spark plug electrode. Spark plugs were analyzed in two typical configurations of the ignition system. A number of tests were conducted to determine the wear of the spark plug electrode exposed to different types of impurities. The spark discharge energy for new and worn spark plugs was determined through calculation.

Key words: electrode burning, fuel mixture impurities, ignition system, spark plugs

1. Introduction

The dynamics of a modern ignition system is difficult to characterize because results obtained from analysis and digital simulations differ from experimental data [1-3]. This paper attempts to determine the impact of fuel impurities on the spark discharge energy and the wear of the spark plug electrode.

Proper operation of a vehicle is largely dependent on the appropriate selection of parameters for its electrical devices. The function of the ignition system is to provide the required spark discharge energy and, as a result, reduce fuel consumption and toxic emissions. It is thus vital that a discharge be of high frequency, high stability and sufficient duration [2, 4, 5]. Due to the presence of anti-detonation additives in fuel, certain amounts of the combustion products may accumulate on the spark plug insulator, and consequently, reduce the discharge energy or even prevent ignition of the mixture. Research on the subject conducted in many centres all over the world aims to optimize the operation of the ignition system by eliminating mechanical elements [6-9].

The ignition system of an internal combustion engine is used to initiate the process of combustion of the fuel-air mixture through an electric discharge at the spark plug. A discharge occurs when the voltage supplied to the plug electrodes is high enough to ionize the gas filling the gap and cause a spark to pass between the electrodes.

A spark discharge consists of:

– a capacity discharge – a very short high-current pulse,

– an induction discharge – a long low-current arc discharge.

The combustion of the fuel-air mixture filling the combustion chamber is largely dependent on the spark discharge parameters determined by the way the discharge is produced [5-7, 10-14] This paper attempts to analyze the system by simulating the effect of fuel impurities on the value of spark discharge energy [1-3, 11-15].

The investigations were conducted in two stages. First, digital simulations of the operation of the ignition system were performed, and then the simulation results were compared with the data obtained for a real ignition system.

During the combustion process, the elements responsible for the ignition of the fuel-air mixture are exposed to strong corrosive action of the combustion products. It is possible to extend the service life of spark plugs by applying special metals or metal alloys resistant to high-temperature corrosion to be welded to the tips of the electrodes. The special metals include iridium, yttrium, platinum and their alloys, for example, platinum-iridium alloys. Some of the latest projects initiated at the Laser Processing Research Centre of the Kielce University of Technology aim to determine whether it is possible to apply solid iridium tips to increase the service life of spark plugs.

2. Model of the ignition system

Generally, ignition systems can be represented as systems accumulating energy in inductance and capacity components [2]. Figure 1 presents a general diagram of a mathematical model, where R_{ls} is the spark plug and C_{45} and R_{45} denote their capacity and resistance, respectively.

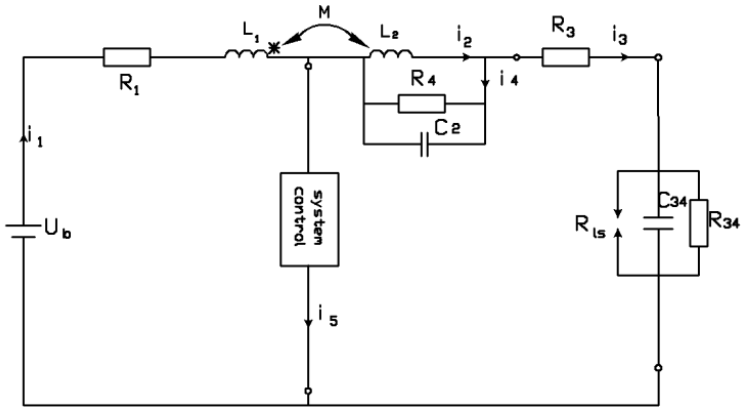

Fig. 1. Model of the ignition system for the simulation studies. U_b – battery voltage, R_1 – resistance of the ignition coil primary winding, L_1 – inductance of the ignition coil primary winding, L_2 – inductance of the ignition coil secondary winding, R_2 – resistance of the ignition coil secondary winding, R_4 – resistance representing the losses in the coil core, R_3 – radioelectrical interference resistance, R_{45} – flow resistance of the spark plug, R_{ls} – discharge resistance, C_2 – self-capacity of the coil, C_{45} – self-capacity of the spark plug, M – coupling

The equivalent circuit of the ignition system presented in Fig. 1 is described by Eqs. (1) and (6) for two states of the control block. The solution to the system of equations obtained for the control block in the contact state by using the state variable method is presented as relationship (4), where it is assumed that the initial conditions, i.e. at the first switch-on, are zero.

$$\begin{aligned}
&U_B - i_1R_1 - L_1\frac{di_1}{dt} + M\frac{di_2}{dt} = 0,\\
&L_2\frac{di_2}{dt} - M\frac{di_1}{dt} + i_2R_2 + i_3R_3 + u_{C45} = 0,\\
&u_{C2} = L_2\frac{di_2}{dt} - M\frac{di_1}{dt} + i_2R_2,\\
&u_{C2} = i_{R4}R_4,\\
&i_3 = i_2 + i_{R4} + i_{C2},\\
&i_3 = i_{R45} + i_{C45},\\
&u_{C45} = i_{R45}R_{45},\\
&i_{C2} = C_2\frac{du_{C2}}{dt},\\
&i_{C45} = C_{45}\frac{du_{C45}}{dt}.
\end{aligned} \tag{1}$$

By introducing state variables: $x_1 = i_1$, $x_2 = i_2$, $x_3 = u_{C2}$, $x_4 = u_{C45}$ to the Eq. (1):

$$\begin{aligned}
&U_B - x_1R_1 - L_1\frac{dx_1}{dt} + M\frac{dx_2}{dt} = 0,\\
&L_2\frac{dx_2}{dt} - M\frac{dx_1}{dt} + x_2R_2 + R_3\frac{x_4}{R_{45}} + R_3C_{45}\frac{dx_4}{dt} + x_4 = 0,\\
&x_3 = L_2\frac{dx_2}{dt} - M\frac{dx_1}{dt} + x_2R_2,\\
&\frac{x_4}{R_{45}} + C_{45}\frac{dx_4}{dt} = x_2 + \frac{x_3}{R_4} + C_2\frac{dx_3}{dt}.
\end{aligned} \tag{1a}$$

Transforming the system of Eq. (1a), we obtain:

$$\begin{aligned}
\frac{dx_1}{dt} &= A_1x_1 + B_1x_2 + C_1x_3 + D_1U_B,\\
\frac{dx_2}{dt} &= A_2x_1 + B_2x_2 + C_2x_3 + D_2U_B,\\
\frac{dx_3}{dt} &= A_3x_1 + B_3x_2 + C_3x_3 + E_3x_3 + D_3U_B,\\
\frac{dx_4}{dt} &= A_4x_1 + B_4x_2 + C_4x_3 + E_4x_4 + D_4U_B,
\end{aligned} \tag{2}$$

where the parameters are determined using the following relationships:

$$C_1 = -\frac{M}{L_2\left(\frac{M^2}{L_2} - L_1\right)}, \qquad D_1 = -\frac{1}{\left(\frac{M^2}{L_2} - L_1\right)},$$

$$A_2 = \frac{-MR_1}{L_1\left(L_2 - \frac{M^2}{L_1}\right)}, \qquad B_2 = \frac{-R_2}{\left(L_2 - \frac{M^2}{L_1}\right)},$$

$$C_2 = \frac{1}{\left(L_2 - \frac{M^2}{L_1}\right)}, \qquad D_2 = \frac{M}{L_1\left(L_2 - \frac{M^2}{L_1}\right)},$$

$$A_3 = \frac{C_{45}A_4}{C_2}, \quad B_3 = \left(\frac{C_{45}B_4}{C_2} - \frac{1}{C_2}\right), \quad C_3 = \left(\frac{C_{45}C_4}{C_2} - \frac{1}{C_2}\right),$$

$$D_3 = \frac{C_{45}}{C_2}D_4U_B, \quad E_3 = \left(\frac{1}{C_2R_{45}} + \frac{C_{45}E_4}{C_2}\right),$$

$$A_4 = \left(\frac{MA_1}{2R_3C_{45}} - \frac{L_2A_2}{2R_3C_{45}}\right), \quad B_4 = \left(\frac{MB_1}{2R_3C_{45}} - \frac{L_2B_2}{2R_3C_{45}} + \frac{R_2}{2R_3C_{45}}\right),$$

$$C_4 = \left(\frac{MC_1}{2R_3C_{45}} - \frac{L_2C_2}{2R_3C_{45}}\right), \quad D_4 = \frac{-L_2D_2}{2R_3C_{45}}, \quad E_4 = -\left(\frac{R_3}{2R_3C_{45}R_{45}} + \frac{1}{2R_3C_{45}}\right).$$

The solution to Eq. (2) has the form:

$$x = \begin{bmatrix} x_1 \\ x_2 \\ x_3 \\ x_4 \end{bmatrix}, \quad A = \begin{bmatrix} A_1 & B_1 & C_1 & 0 \\ A_2 & B_2 & C_2 & 0 \\ A_3 & B_3 & C_3 & E_3 \\ A_4 & B_4 & C_4 & E_4 \end{bmatrix}, \quad B = U_B\begin{bmatrix} D_1 \\ D_2 \\ D_3 \\ D_4 \end{bmatrix}. \tag{3}$$

At the first switch-on, the initial conditions are zero and Eq. (3) assumes the form:

$$\frac{d}{dt}x = Ax + B, \qquad x = e^{At}x_0 + \int_0^t e^{A(t-\tau)}Bd\tau,$$
$$x = \int_0^t e^{A(t-\tau)}Bd\tau. \tag{4}$$

The solution to the system of equations obtained for the control block in the non-contact state by using the state variable method is presented as relationship (7), where the initial conditions, i.e. the final conditions from the previous state, need to be calculated from the formulae for the control block in the contact state for the time equal to the time of contact.

$$
\begin{aligned}
&U_B - i_3 R_1 - L_1 \frac{di_3}{dt} + M \frac{di_2}{dt} - L_2 \frac{di_2}{dt} + M \frac{di_3}{dt} - i_3 R_3 - u_{C45} = 0,\\
&u_{C2} = L_2 \frac{di_2}{dt} - M \frac{di_3}{dt} + i_2 R_2,\\
&u_{C2} = i_{R4} R_4,\\
&i_3 = i_2 + i_{R4} + i_{C2},\\
&i_3 = i_{R45} + i_{C45},\\
&u_{C45} = i_{R45} R_{45},\\
&i_{C2} = C_2 \frac{du_{C2}}{dt},\\
&i_{C45} = C_{45} \frac{du_{C45}}{dt}
\end{aligned}
\tag{5}
$$

In this case, the unknowns are: i_2, i_3, i_{R4}, i_{C2}, i_{R45}, i_{C45}, u_{C2}, and u_{C45}.
By introducing state variables: $x_1 = i_2$, $x_2 = i_3$, $x_3 = u_{C2}$, $x_4 = u_{C45}$ to the Eq. (5):

$$
\begin{aligned}
&U_B - x_2(R_1 + R_3) + (M - L_1)\frac{dx_2}{dt} + (M - L_2)\frac{dx_1}{dt} - x_4 = 0,\\
&x_3 = L_2 \frac{dx_1}{dt} - M \frac{dx_2}{dt} + x_1 R_2 \rightarrow \frac{dx_2}{dt} = \frac{L_2}{M}\frac{dx_1}{dt} + x_1 \frac{R_2}{M} - \frac{1}{M} x_3,\\
&x_2 = x_1 + \frac{x_3}{R_4} + C_2 \frac{x_3}{dt} \quad \rightarrow \quad C_2 \frac{x_3}{dt} = -x_1 + x_2 - \frac{x_3}{R_4},\\
&x_2 = \frac{x_4}{R_{45}} + C_{45} \frac{dx_4}{dt} \quad \rightarrow \quad C_{45} \frac{dx_4}{dt} = x_2 - \frac{x_4}{R_{45}}.
\end{aligned}
\tag{5a}
$$

Transforming the system of Eqs. (5), we obtain:

$$
\begin{aligned}
&\frac{dx_1}{dt} = a_1 x_1 + b_1 x_2 + c_1 x_3 + d_1 x_4 + e_1 U_B,\\
&\frac{dx_2}{dt} = a_2 x_1 + b_2 x_2 + c_2 x_3 + d_2 x_4 + e_2 U_B,\\
&\frac{dx_3}{dt} = a_3 x_1 + b_3 x_2 + c_3 x_3,\\
&\frac{dx_4}{dt} = b_4 x_2 + d_4 x_4.
\end{aligned}
\tag{6}
$$

For the system of Eqs. (6) the parameters $a_1 - d_4$ are defined by the relationships:

$$a_1 = -\frac{R_2(M-L_1)}{[L_2(M-L_1)+M(M-L_2)]}, \qquad b_1 = \frac{M(R_1+R_3)}{[L_2(M-L_1)+M(M-L_2)]},$$

$$c_1 = \frac{(M-L_1)}{[L_2(M-L_1)+M(M-L_2)]}, \qquad d_1 = \frac{M}{[L_2(M-L_1)+M(M-L_2)]}, \qquad e_1 = -d_1,$$

$$a_2 = \frac{a_1L_2+R_2}{M}, \; b_2 = \frac{b_1L_2}{M}, \quad c_2 = \frac{c_1L_2-1}{M}, \quad d_2 = \frac{d_1L_2}{M}, \quad e_2 = -\frac{e_1L_2}{M},$$

$$a_3 = -\frac{1}{C_2}, \quad b_3 = \frac{1}{C_2}, \quad c_3 = -\frac{1}{C_2R_4}, \quad b_4 = \frac{1}{C_{45}}, \quad d_4 = -\frac{1}{C_{45}R_{45}}.$$

The solution to Eq. (6) has the form:

$$x = \begin{bmatrix} x_1 \\ x_2 \\ x_3 \\ x_4 \end{bmatrix}, \qquad A = \begin{bmatrix} a_1 & b_1 & c_1 & d_1 \\ a_2 & b_2 & c_2 & d_2 \\ a_3 & b_3 & c_3 & 0 \\ 0 & b_4 & 0 & d_4 \end{bmatrix}, \qquad B = U_B \begin{bmatrix} e_1 \\ e_2 \\ 0 \\ 0 \end{bmatrix}, \tag{7}$$

$$\frac{d}{dt}x = Ax + B, \qquad x = e^{At}x_0 + \int_0^t e^{A(t-\tau)}Bd\tau,$$

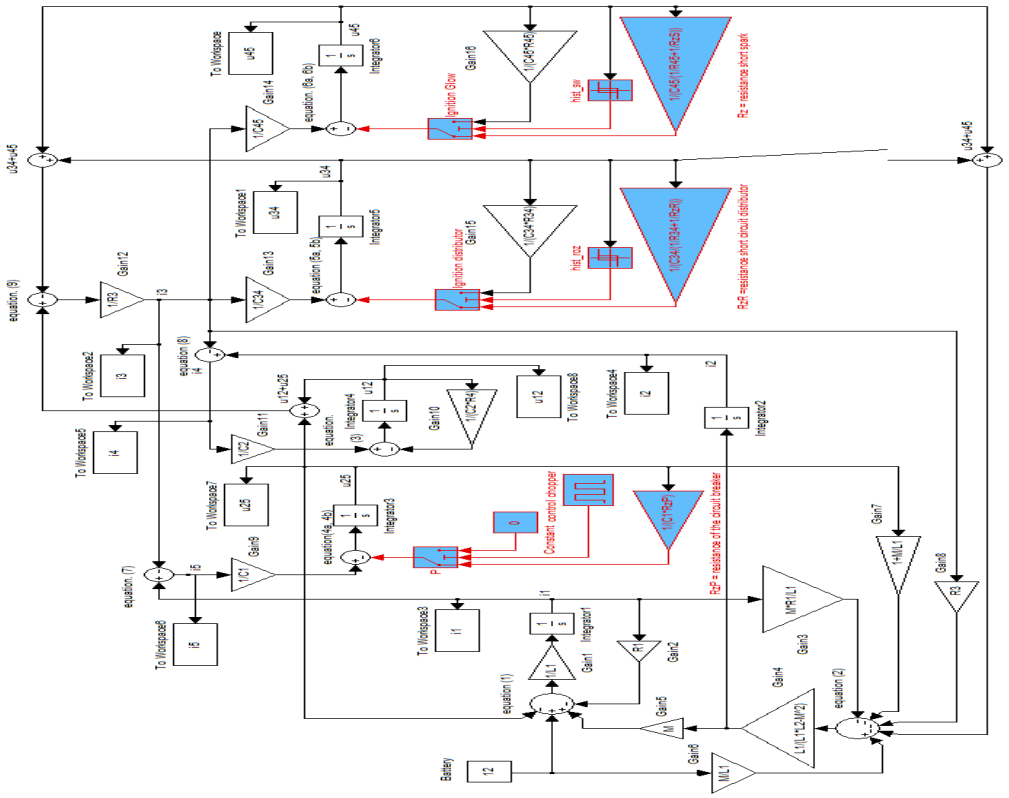

Fig. 2. Operating diagram of the ignition system to implement the spark discharge in Simulink

where x_0 defines initial conditions, or final conditions from the previous state, to be calculated from the formulae for the control block in the contact state for the time equal to the time of contact.

The time t will be counted from the moment the block it no longer in the contact state.

The spark discharge energy is dependent on a number of factors, including the parameters of the ignition primary circuit.

3. The effect of fuel impurities on the wear of the spark plug electrodes-operational research

The investigations performed under real operating conditions involved observing the microscopic gap between the spark plug electrodes before the tests and after every five hours of operation. The tests were carried out using a specially built setup presented in Fig. 3.

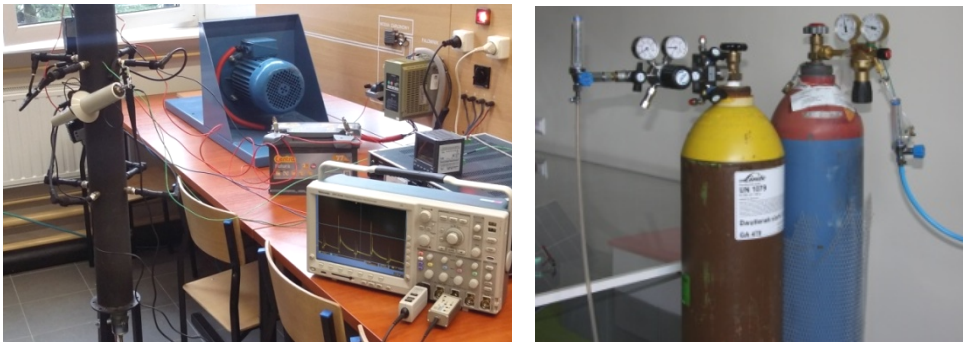

Fig. 3. A setup to test ignition systems

The microscopic analysis was conducted at the Electrical Discharge Machining Laboratory of the Laser Processing Research Centre using a Hirox KH-8700 digital microscope. The device is able to magnify objects from 35 to 5000 times; it can also perform measurements and display surface profiles.

The experimental setup can be used to simulate the conditions in the combustion chamber. As shown in the photograph, the vertical combustion chamber has spark plugs mounted at three levels. When combined with the throttle in the exhaust port, they enable us to adjust the temperature at which a spark will jump between the electrodes. The setup is also capable of providing a precise amount of fuel. The amount of fuel is measured using appropriate rotameters. The fuel tested was pure methane (CH4) or methane contaminated with sulphur dioxide (SO2).

The fuel contaminant was selected intentionally because sulphur compounds are naturally present in each type of biogas that requires further processing. Sulphur compounds present in the fuel mixture are responsible for the acidification of the system, which results in spark plug deterioration, for example, the wear of nickel electrodes (with no tips made of refractory materials) due to erosion.

There is an increase in the gap, which makes it extremely difficult for a spark to jump between the electrodes. This leads to the occurrence of the so-called 'no ignition spark', not being able to initiate the combustion process.

The tests were conducted at the same electrical parameters for different fuel mixture compositions. This paper presents results obtained for the combustion of pure methane and methane contaminated with sulphur dioxide (5% by volume). In both cases, the combustion process was sustained by applying atmospheric air as an oxidizing agent. The temperature inside the combustion chamber was circle 400°C.

The images below show selected results of the tests conducted for fuel with different contents of sulphur dioxide as a contaminant.

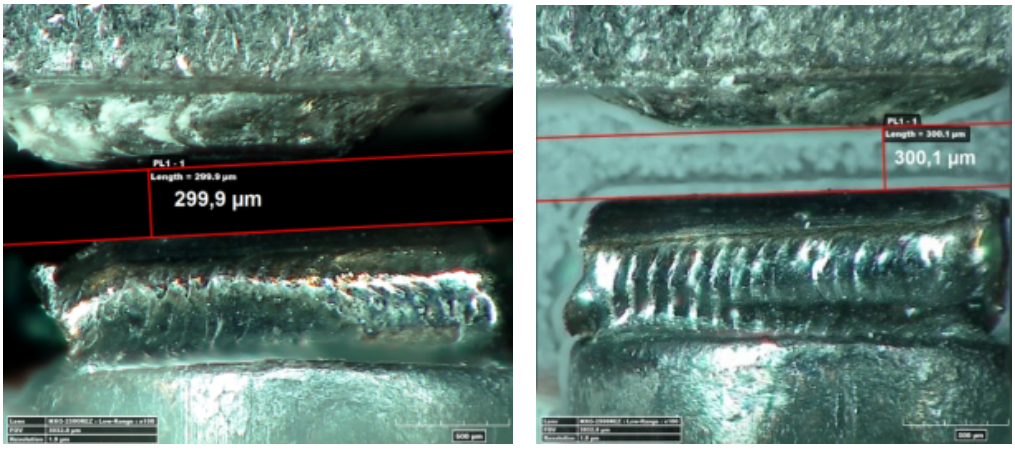

Fig. 4. View of the gap before the test; left: non-contaminated spark plug; right: spark plug contaminated with fuel containing 5% by volume of sulphur dioxide

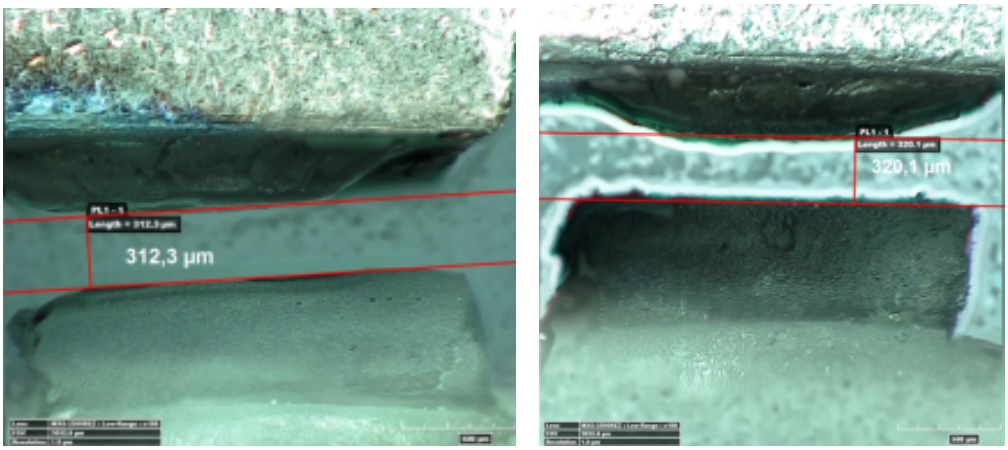

Fig. 5. View of the gap after 800 h of operation; left: non-contaminated spark plug; right: contaminated spark plug

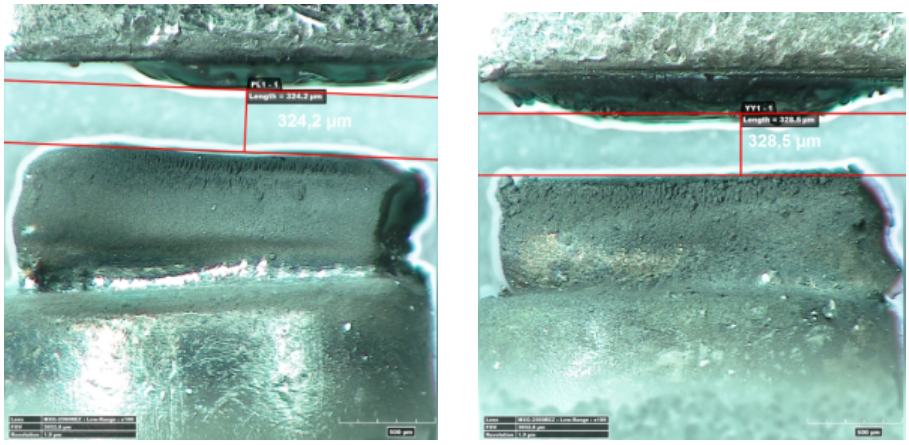

Fig. 6. View of the gap after 1400 h of operation; left: non-contaminated spark plug; right: contaminated spark plug

4. Determination of the spark discharge energy for different types of electrodes

The discharge energy recorded for a capacitor ignition system was 32.60 mJ when new ISKRA spark plugs (Fig. 4.) were used. In the case of spark plugs with an 800-hour service life (Fig. 5.), the level of energy remained the same when non-contaminated fuel was used; however, it decreased to 26.25 mJ when fuel contaminated with sulphur dioxide was applied. Spark plugs with a service life of 1400 h (Fig. 6.) transmitted 32.30 mJ of energy when non-contaminated fuel was used. However, when the fuel was contaminated, the amount of energy available for ignition was 23.20 mJ.

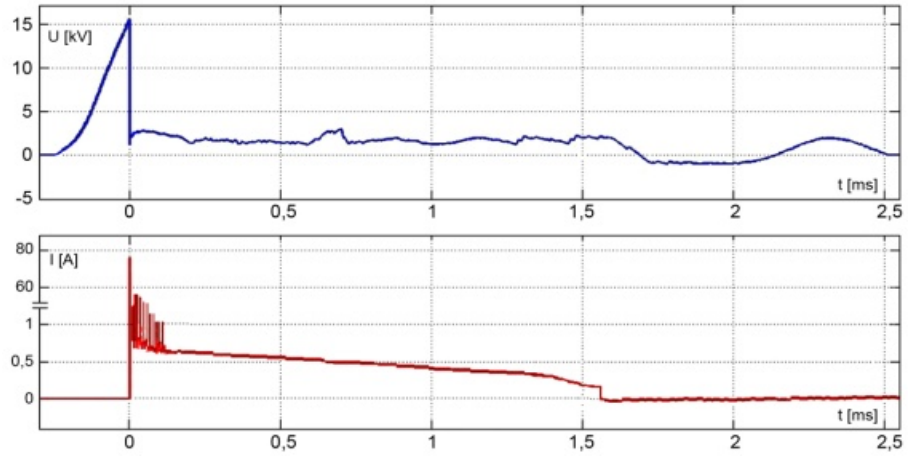

Fig. 7. Current and voltage for a new spark plug, E = 33.1 mJ – computer simulation

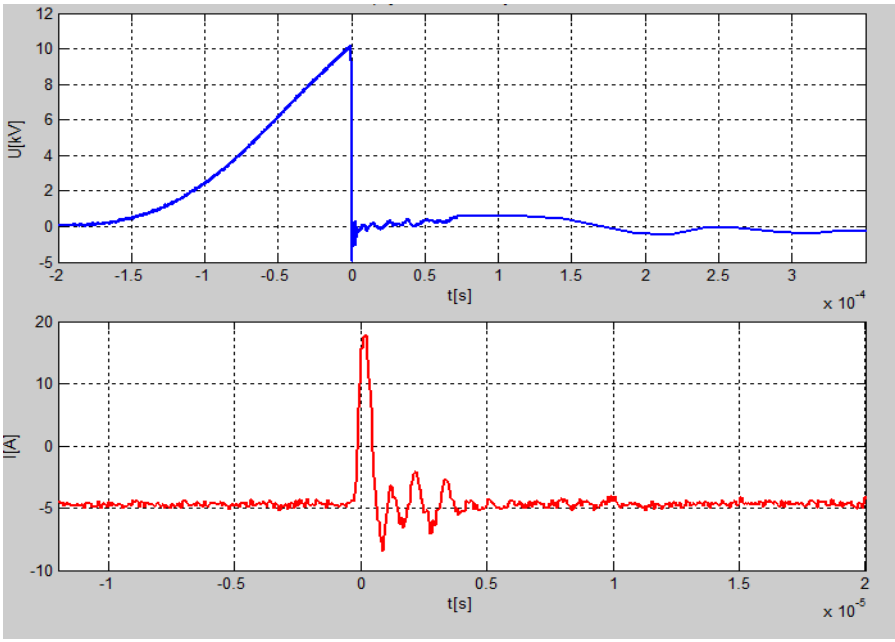

Fig. 8. Current and voltage for a new spark plug, E = 32.6 mJ – laboratory tests (capacity spark discharge)

For spark plugs with an 800-hour service life, the energy obtained at the capacitor discharge was E=26.25 mJ (Fig. 10.)

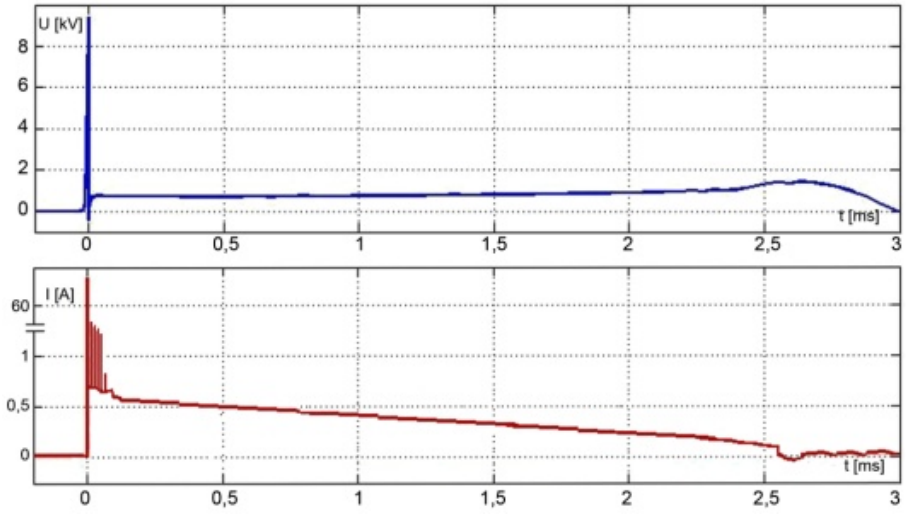

Fig. 9. Current and voltage for a spark plug with an 800-hour service life, E=26.85 mJ – computer simulation.

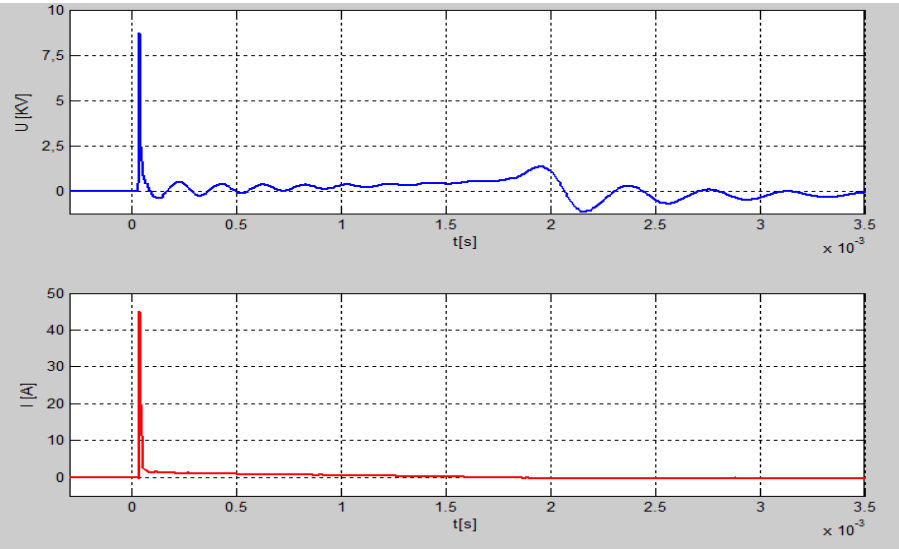

Fig. 10. Current and voltage for a spark plug with an 800-hour service life, E = 26.25 mJ – laboratory tests (capacity spark discharge)

5. Conclusions

The test results indicate that the wear of the electrodes operating in a contaminated environment was higher. The distance between the central and side electrodes increased at each stage of the measurement process. Finally, there were more products of incomplete fuel combustion present on the surface of the electrodes when these were tested under contaminated conditions.

The laboratory-based experimental data verified by means of the computer simulation results show that the amount of energy released as a spark discharge is largely dependent on the quality of fuel supplied to the engine and the resultant wear of the spark plug electrodes.

As can be seen, the wear of the spark plug electrode has a considerable effect on the amount of the spark discharge energy.

Acknowledgements

The research was supported by the National Centre for Research and Development (NCBiR), project no. PBS1/B5/13/2012.

References

[1] Herner A., Riehl H.J., *Analysis of the impact of design solutions and parameters of the ignition system at the spark discharge energy value (in Polish)*, Warszawa (2003).

[2] Różowicz S., *Analysis of the impact of design solutions and parameters of the ignition system at the spark discharge energy value. The doctoral dissertation (in Polish)*, PŚK (2012).

[3] Stone C, Brown A, Beckwith P., Cycle-by-Cycle *Variations in Spark Ignition Engine Combustion – part II: Modeling of Flame Kernel Displacements as a Cause of Cycle-by-Cycle Variations*, SAE paper 960613 (1996).
[4] Robinet C, Andrzejewski J, Higelin P. *Cycle-to-Cycle Variation Study of an SI Engine Fired by Spark Plug and a Non Conventional Device*, SAE paper 972986 (1997).
[5] Hunicz J., Wac E., Kabała J., *Comparative studies of new construction of spark plugs (in Polish)*, 3 (2006).
[6] Alger T, Mangold B, Mehta D, Roberts C., *The effect of Sparkplug Design on Initial Flame Kernel Development and Sparkplug Performance*, SAE paper (2006).
[7] Ezekoye D., Hall M., Matthews R., *Railplug Ignition System for Enhanced Engine Performance and Reduced Maintenance*, USA (2005).
[8] Han S., *Investigation of Cyclic Variations of IMEP under Idling Operation in Spark Ignition Engines*, KSME International Journal (2001).
[9] Herweg R, Ziegler G.F.W., *Flame Kernel Formation in a Spark-ignition Engine,* International symposium COMODIA 90: 173-178 (1990).
[10] Kaniewski J., Fedyczak Z., *Modeling and Analysis of Dynamic Properties of the Hybrid Transformer with MRC*, Przegląd Elektrotechniczny, 87(1): 45-50 (2011).
[11] Kubiak P., Zalewski M., *Laboratory diagnosis of motor vehicles (in Polish)*, WKŁ (2012).
[12] Lee K, Kim K., *Influence of Initial Combustion in SI Engine on Following Combustion Stage and Cycle-by-cycle Variations in Combustion Process*, The International Journal of Automotive Technology, 2(1): 25-31 (2001).
[13] Lee Y, Boehler J., *Flame Kernel Development and Its Effects on Engine Performance with Various Spark Plug Electrode Configurations*, SAE paper 2005-01-1133 (2005).
[14] Lee Y, Grimes D, Boehler J, Sparrow J, Flavin C., *A Study of the Effects of Spark Plug Electrode Design on 4-cycle Spark-ignition Engine Performance*, SAE paper 2000-01-1210 (2000).
[15] Osamura H., *Development of Long Life and High Ignitability Iridium Spark Plug,* FISITA World Automotive Congress, Paper number F2000A144, Korea (2000).